

Efficient comparison of path-lengths using Fourier multipoint devices

J A Dunningham¹ and A Vourdas²

¹ School of Physics and Astronomy, University of Leeds, Leeds LS2 9JT, UK

² Department of Computing, University of Bradford, Bradford BD7 1DP, UK

Received 22 September 2005, in final form 1 February 2006

Published 8 March 2006

Online at stacks.iop.org/JPhysB/39/1579

Abstract

We present a scheme for comparing effective path-lengths through a spatial region by using multipath generalizations of a Mach–Zehnder interferometer. This enables us to identify paths that have different lengths from the others with exponentially fewer measurements than would be required by repeated measurements with a standard two-path interferometer. We show that this scheme is extremely sensitive to small variations in the paths, which means it could be used to measure the variance of the path-lengths accurately and efficiently. Possible applications include accurately measuring spatial variations of potential fields and efficiently identifying which of many cavities contains an atom.

The advent of interferometers allowed unprecedented levels of precision to be achieved in optical measurements. For the first time, path-length differences could be measured to within a small fraction of the wavelength, λ , of light. This dramatic improvement in resolution has kept interferometers at the forefront of a wide range of technological applications, particularly in the field of metrology.

Ever since their inception, a great deal of effort has been devoted to enhancing the resolution of interferometers further still. One way this can be achieved is to use number-squeezed light as the input [1–3]. For coherent light (i.e. light that is not squeezed), the path-length difference can be measured to within λ/\sqrt{N} , where N is the mean number of photons. By using perfectly number-squeezed light at the input, it is possible to substantially improve the resolution to λ/N . Another proposal for improving the resolution is to increase the number of paths through the interferometer. A standard Mach–Zehnder interferometer has two paths; by increasing this to d paths, the resolution scales as $\lambda/(d\sqrt{N})$ [4]. This strategy is analogous to a diffraction grating, which enables better phase resolution than a double slit set-up, by increasing the number of possible paths the light can take.

In order to create multipath interferometers we need multipoint generalizations of beam splitters. These multipoint beam splitters are equivalent to so-called Fourier multipoint devices, which relate the annihilation and creation operators at the output ports to those at the input ports through a finite Fourier transform. A significant body of work has been devoted to

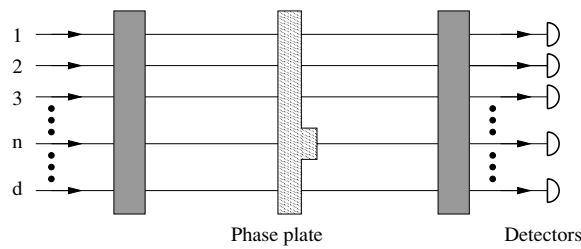


Figure 1. Scheme for identifying the anomalous path. A multipath interferometer is created by arranging two $2d$ -multiport devices, which are inverses of each other, in sequence with a region of evolution between them. One of the paths has a phase shift relative to the others—schematically represented by a phase plate with a ‘kink’ in it. By passing a coherent state into one input port and detecting particles at the outputs, it is possible to efficiently identify which path has the phase shift.

the formalism of these devices [5–8] and interest in them has increased rapidly as they have become physically implementable. Multiport beam splitters with six or eight ports have been experimentally demonstrated using photons and ordinary beam splitters [9] and there are suggestions for how these could be scaled up to larger systems [5]. They can also be made by splicing optical fibres and such constructions are commercially available with up to 32 input and output ports [10]. Experiments with Bose–Einstein condensates trapped in optical lattices also suggest an interesting new avenue for their realization with atoms [11, 12]. A multipath interferometer is then constructed by combining two multiport beam splitters in much the same way that a Mach–Zehnder interferometer is constructed from two ordinary beam splitters.

In this paper, we build upon previous work on multipath interferometers and demonstrate a different application for them. Instead of using them to make high-precision measurements of phase shifts [4] or to generate entanglement for quantum protocols [10, 13–15], we discuss how they can be used to compare the path-lengths (or equivalently phase shifts) through some spatial region. We begin by demonstrating how we can efficiently identify which (of many) paths contains a phase shift relative to the others. This could, for example, be used to determine which of many cavities or traps contained an atom and so could be useful as a read-out mechanism for quantum information schemes.

If we were to use standard two-path interferometry, finding the anomalous path would entail directly measuring the length of each path individually. Here we demonstrate a scheme that requires exponentially fewer measurements. In the second part of this paper, we consider the effects of small path-length variations on the system and show that our scheme is acutely sensitive to them. We show how this apparent weakness can be turned to a strength if we are interested in measuring the variance of the path-lengths through some region of space. This could be applied, for example, to accurately measuring spatial variations of a potential field. Related proposals use entanglement to efficiently compare quantum states [16, 17] and to determine whether two unitary functions are the same [18].

The system we consider (see figure 1) consists of a $2d$ -port Fourier device, with d inputs and d outputs, followed by a region of evolution and another $2d$ -port Fourier device, which performs the inverse transform of the first one. This setup can be thought of as a multipath Mach–Zehnder interferometer. A detailed discussion of the operation of this device is provided elsewhere [5].

As the input to the system we take a coherent state at port j with amplitude $\sqrt{d}\beta$ and vacuum states at all the other ports. The mean total number of particles in the input is

$N_{\text{tot}} = d|\beta|^2$ and the state can be written as

$$|\psi\rangle = |0, 0, \dots, \sqrt{d}\beta, \dots 0\rangle_a, \quad (1)$$

in the basis of the input ports. The action of a Fourier multiport device is to transform the input annihilation operators $\{a_1, a_2, \dots, a_d\}$ to the output annihilation operators $\{A_1, A_2, \dots, A_d\}$ according to [5]

$$A_m = \frac{1}{\sqrt{d}} \sum_{k=1}^d a_k \omega^{km}, \quad (2)$$

where $\omega = \exp(i2\pi/d)$.

The first multiport device transforms (1) to give

$$|\Psi\rangle = |\beta\omega^j, \beta\omega^{2j}, \dots, \beta\omega^{dj}\rangle_A, \quad (3)$$

as the state at the output ports. We see that the initial coherent state has been equally split between all the outputs. This means that each path is scanned simultaneously before the state is recombined at the second multiport device.

Next we assume that all the path-lengths are the same except one. This irregular path may have a different refractive index due to the presence of other particles, have a different spatial length, or a different energy. Whatever the cause, the effect will be a phase shift, ϕ , of this path relative to the others. This is represented schematically in figure 1 by the insertion of a phase plate with a ‘kink’ in one path. It is this anomalous path that we wish to identify by our scheme. Without loss of generality, we take the phase shift to be in path n . Mathematically this is achieved with the operator $\exp(i\phi A_n^\dagger A_n)$ acting on state (3). This gives

$$|\Psi\rangle = |\beta\omega^j, \dots, \beta\omega^{nj} e^{i\phi}, \dots, \beta\omega^{dj}\rangle_A. \quad (4)$$

Finally, we transform the state through a second Fourier device, which performs the inverse transform of the first device. This completes the multipath interferometer. If the inputs to the second multiport device are the coherent states $|\{\beta_k\}\rangle$, the outputs are the coherent states $|\{B_l\}\rangle$ given by [5]

$$B_l = \sum_{k=1}^d (F^{-1})_{lk} \beta_k, \quad (5)$$

where

$$(F^{-1})_{lk} = d^{-1/2} \omega^{-lk}. \quad (6)$$

Substituting (6) into (5) and using (4) for the values of $\{\beta_k\}$, we can calculate the outputs from the interferometer. This gives

$$\begin{aligned} B_l &= \frac{\beta}{\sqrt{d}} \left(\sum_k \omega^{-k(l-j)} - \omega^{-n(l-j)} + \omega^{-n(l-j)} e^{i\phi} \right) \\ &= \frac{\beta}{\sqrt{d}} (d\delta_{l,j} + (e^{i\phi} - 1)\omega^{-n(l-j)}), \end{aligned} \quad (7)$$

where $\delta_{l,j}$ is the Kronecker delta function and has the value 1 when $l = j$ or 0 when $l \neq j$. As our measurement, we simply detect the number of particles at each output port. The mean number is given by

$$|B_j|^2 = |\beta|^2 \left[d - 2 \left(1 - \frac{1}{d} \right) (1 - \cos \phi) \right] \quad (8)$$

$$|B_{l \neq j}|^2 = 2 \frac{|\beta|^2}{d} (1 - \cos \phi). \quad (9)$$

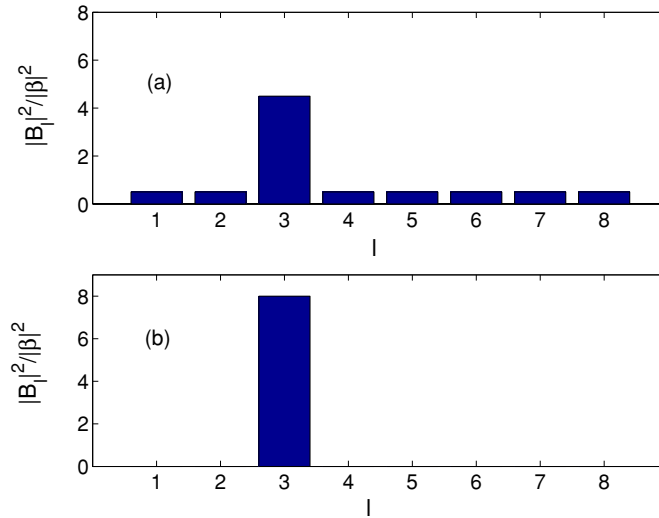


Figure 2. Mean output number at each port (labelled l) for an input coherent state at port 3 with (a) a relative phase shift of π in one path and (b) all paths identical.

There will be fluctuations of order $|B_l|$ in the number of particles detected at port l between runs. For sufficiently large amplitudes, we can ignore these fluctuations since they will be a small fraction of the mean number detected.

For no phase shift, $\phi = 0$, all the particles emerge in port j as we would expect. We can optimize the effect of the phase shift by picking $\phi = \pi$, i.e., the path-length difference is half the wavelength of the incident light. This gives

$$|B_j|^2 = |\beta|^2 \left[d - 4 \left(1 - \frac{1}{d} \right) \right] \quad (10)$$

$$|B_{l \neq j}|^2 = 4|\beta|^2/d. \quad (11)$$

This operation conserves the total number of particles as it should. The effect of a phase shift in one path is to remove particles from output port j and to place them in a uniform distribution across the other ports (see figure 2). It can be seen from (10) and (11) that the output distribution does not depend on n , i.e., it is independent of which path contains the phase shift. This is not surprising since the symmetry of the system means that all paths are equivalent.

At first sight, the fact that the output is independent of which path contains the shift suggests that this technique will not enable us to identify that path. However, what it can tell us is whether or not one of the paths is different from the others. This is clear by comparing the plots in figure 2, which show the output distributions when there is (figure 2(a)) and is not (figure 2(b)) a phase shift in one path. We see from this that the (small) fluctuations in the output numbers are not important since any non-zero population in the ports $l \neq j$ gives evidence of a phase shift. A similar argument reveals that this scheme is only weakly affected by non-unit detector efficiencies at the output ports [4]. Furthermore, any stray particles in the vacuum input ports will simply give an additional background at the output ports. This effect can be neglected if the mean number of stray particles at each input is much less than $4|\beta|^2/d$, i.e., the population at output ports $l \neq j$ due to the phase shift. We now show how this scheme can be exploited to efficiently identify the anomalous path.

Suppose we have $d = 2^p$ input ports, where p is a positive integer. We begin by performing the interferometry scheme outlined above and measuring the population in the output ports. A ‘plateau’ in the ports $l \neq j$ of the form shown in figure 2(a) confirms that there is phase shift in one of the paths and enables us to determine the magnitude of that phase shift (modulo 2π). Next we repeat the interferometry scheme but this time for only half of the paths, for example the first 2^{p-1} ports. Since the phase shift is in only one of the paths, the result of this measurement will have the general form of either figure 2(a) or 2(b) depending on whether or not the phase shift is in one of the paths that we have chosen. Either way, this will enable us to know which half the shift is in and, in a single measurement, the search space is halved.

We can, of course, repeat this procedure another $(p - 2)$ times. Each time we halve the search space and so after a total of p measurements (including the one before we started halving) we have narrowed the search space down to two possibilities. At this point we cannot continue the halving procedure since we need at least two paths for an interferometer. However, given that we know ϕ from the first measurement, we can shift the phase of one path by $-\phi$ and then perform one final interferometry measurement. If we add it to the path that had the original phase shift, both paths will now have the same path-lengths and the output will all be in one port. Otherwise the output particles will be divided between both output ports. Either way, this now definitively identifies which path has the phase shift.

In summary, for $d = 2^p$ paths, this technique can find the path containing the phase shift with only $(p + 1)$ measurements, i.e., the number of required measurements scales as $\mathcal{M} \sim \log_2 d$. This offers an exponential improvement in efficiency when compared with two-path interferometry, which requires on average 2^{p-1} measurements. The power of this technique lies in the fact that it scans all the paths simultaneously. This means that the state is changed if there is a phase shift in any path and this manifests itself as the tell-tale ‘plateau’ in the number distribution when the paths are recombined.

This scheme can also be applied to systems with more than one anomalous path. For example, suppose there were phase shifts in two arms, n and q , of the interferometer. As before, we take the input to be a coherent state in one port and vacua in all the others and, for simplicity, take both phase shifts to have the value $\phi = \pi$. The mean populations of particles at the output ports for a 12-path interferometer are shown in figure 3. As before, there is a peak corresponding to the input port—in this case port 3—and some distribution of particles in the other ports. This distribution over the other ports is no longer a plateau, but now depends on the values of n and q , i.e., which arms the phase shifts are in. We have neglected the case $n = q$, since this is covered by the single phase shift analysis above.

We can use this result to identify the anomalous paths by a procedure similar to the one discussed above. We perform the interferometry scheme on half the paths. If both phase shifts are in this measured half, the output distribution will have the general form of one of the plots in figure 3. So long as we can distinguish this from the case that both phase shifts are in the other half, in which case the output is all in one port (figure 2(b)), the search space is halved by a single measurement. We keep iterating this procedure until we reach the case that one of the phase shifts is in each half and we obtain plots of the form of figure 2(a). At this point, we simply apply the single phase shift procedure to each half to unambiguously determine which paths the shifts are in. Again, this can be achieved with an exponential improvement over the two-path case. We may also be able to gain some improvement by distinguishing the outputs shown in figure 3. This would tell us how far apart the two phase shifts are and so further reduce the search space (i.e. if we can identify one shift, the other one is easily found). Of course, to distinguish these different outputs, we require a favourable signal to noise ratio. This could be achieved by using a sufficiently large coherent state as the input. It may also be possible to combine this scheme with proposals for using squeezed state inputs in order to

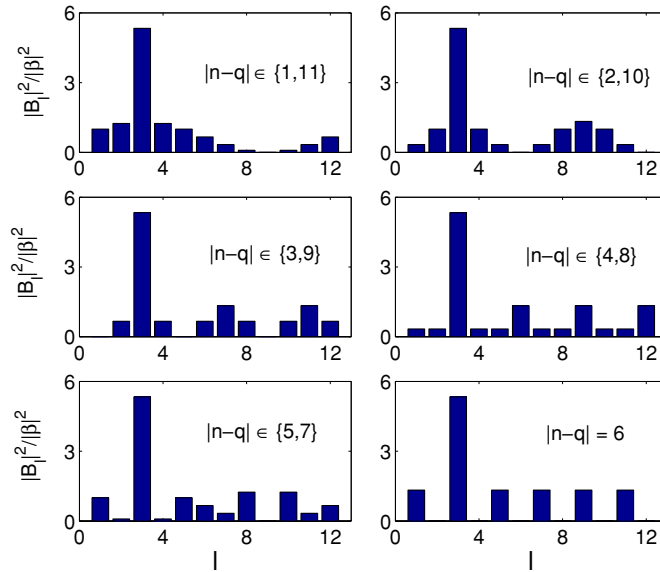


Figure 3. Distributions for the mean number of particles at each output port (labelled l) for a coherent state input at port 3. There are phase shifts of $\phi = \pi$ in two of the paths, n and q . The distribution depends on the value of $|n - q|$.

improve the resolution of the phase shift [1–3]. This does not allow one to find the anomalous path more efficiently, but rather allows one to identify smaller phase shifts and so effectively find smaller ‘needles in the haystack’.

The scheme discussed so far is applicable to systems where we can ignore any classical variation between the paths, i.e., all the non-anomalous paths have exactly the same length. This may apply, for example, to systems where the presence or absence of an atom in a cavity can change the effective path-length through the cavity by a set value. We would now like to consider what happens when the path-length has a continuous range of possible values and the non-anomalous elements do not all have exactly the same value. We emphasize that these are not quantum fluctuations in the paths, but rather classical uncertainties, which we assume do not destroy the quantum superpositions. These latter uncertainties would arise, for example, in the case of a potential field with small spatial variations. To characterize this system we need to account for the phase variations between paths. In particular, we would like to quantify how large these imperfections can be while still enabling us to identify the anomalous path.

Let us write the probability distribution of the phase, ϕ_k , corresponding to the length of path k as $P(\phi_k)$. We take each path to have the same mean path-length and distribution. Averaging over all these variations, the expected number of particles at output port l is given by

$$|B_l|^2 = \frac{|\beta|^2}{d} \int_0^{2\pi} \dots \int_0^{2\pi} P(\phi_1) \dots P(\phi_d) d\phi_1 \dots d\phi_d \left| \sum_{k=1}^d \omega^{-k(l-j)} e^{i\phi_k} \right|^2. \tag{12}$$

If we consider only the output corresponding to the port with the coherent state input, i.e., $l = j$, we obtain

$$|B_j|^2 = |\beta|^2 \left[1 + (d - 1) \left| \int_0^{2\pi} P(\phi) e^{i\phi} d\phi \right|^2 \right]. \tag{13}$$

This is an expression for a general distribution, $P(\phi)$, of phases. We now take the specific case that the variations are normally distributed with mean zero and standard deviation σ ,

$$P(\phi_k) = \frac{1}{\sigma\sqrt{2\pi}} \exp\left[-\frac{\phi_k^2}{2\sigma^2}\right]. \quad (14)$$

Substituting (14) into (13) gives [19]

$$|B_j|^2 = |\beta|^2 [1 + (d-1)e^{-\sigma^2 d}]. \quad (15)$$

For a completely flat distribution of phases ($\sigma^2 \rightarrow \infty$), the mean number of particles at each output port is uniform, as we might expect.

We would now like to determine how large the variations can be while still allowing us to identify that one of the paths has an average phase shift of ϕ . We can see from (8) that a phase shift of ϕ in one path reduces the population detected at output port j by $2|\beta|^2(1-1/d)(1-\cos\phi)$. From (15), the effect of phase variations with variance σ^2 is to reduce the population at port j by $(d-1)|\beta|^2[1-e^{-\sigma^2 d}]$. This means that the effect of the variations is smaller than the effect of the ϕ phase shift when $\sigma^2 < 2(1-\cos\phi)/d^2$, for $d^2 \gg 1$. For the case, $\phi = \pi$, the condition becomes $\sigma^2 < 4/d^2$. This places a severe restriction on the extent to which the path-lengths can vary.

This extreme sensitivity to path-length variations could be viewed as a weakness of this scheme. However, it is turned into a great strength if we are interested in making precise measurements of these variations. This technique could therefore be applied to any system for which we would like to accurately and efficiently compare phase shifts. One possibility is if we wanted to determine the spatial variations of a potential field. This could be achieved by scanning across the path-lengths of each of the d elements of the field using two-path interferometry. If we used N_{tot}/d particles to measure each element, where N_{tot} is the total resource of particles available, the variance in our knowledge of each path-length would scale as d/N_{tot} . Repeating this for the remaining $(d-1)$ elements and combining the results would enable us to determine the variance of the path-length distribution to a resolution that scales as $1/N_{\text{tot}}$. This procedure would require d separate measurements.

By comparison, we could use the multipath interferometry technique outlined above to coherently split a coherent state into d paths which are directed through each of the d elements of the field before being recombined. The population detected at output mode j is given by (15) and so, for $\sigma^2 d \ll 1$, the reduction in population at this port due to the variation of the path-lengths is

$$\Delta|B_j|^2 = -d(d-1)|\beta|^2\sigma^2 \approx -N_{\text{tot}} d\sigma^2. \quad (16)$$

By measuring this quantity it is clear that we could determine the variance, σ^2 , of the path-length variations with a resolution that scales as $1/(dN_{\text{tot}})$. This represents a d -fold improvement over the two-path case. Furthermore, it can be achieved in a single measurement—a significant advantage over the two-path case, which requires d measurements.

An important issue that comes out of this work is the calibration of the interferometer. Thus far, we have assumed that it is possible to achieve a stable multipath interferometer where all the paths are identical (modulo the wavelength of the light used). The scheme for measuring the variance of the paths (outlined above) can be viewed as a read-out of the calibration of the interferometer. If light is fed into only one input port, then if all the light emerges from the corresponding output port, the interferometer is properly calibrated and all the paths have the same optical path-length. This, however, may be difficult to achieve in practice. We now discuss the results when the interferometer is not properly calibrated. If we take the distribution of the path-lengths due to calibration error to be normally distributed with

a variance σ_c^2 , following the discussion above, the expected number of detections at output port j is

$$|B_j|^2 = |\beta|^2 [1 + (d - 1) e^{-\sigma_c^2 d}]. \quad (17)$$

When this uncalibrated interferometer is used to measure the variation of a field with variance σ_f^2 , the output at port j is given by

$$|B_j|^2 = |\beta|^2 [1 + (d - 1) e^{-(\sigma_c^2 + \sigma_f^2)d}]. \quad (18)$$

Therefore, the change in expected population at output port j due to the introduction of the field is

$$\Delta |B_j|^2 \approx -N_{\text{tot}} d \sigma_f^2, \quad (19)$$

if $(\sigma_c^2 + \sigma_f^2)d \ll 1$. This has the same form as (16) and so, in this limit, imperfections in the calibration should not be a major obstacle to the schemes outlined in this paper.

In conclusion, we have highlighted the great potential that Fourier multipoint devices hold by considering their particular application to identifying and characterizing spatial path-lengths. We have shown how multipoint devices enable us to identify an anomalous path with an exponential decrease in the number of measurements required when compared with scanned measurements with two-path interferometers. We have also considered the case where the path-lengths can take a range of values and shown that any slight variations rapidly diminish our ability to distinguish the anomalous path. This great sensitivity opens up the new and interesting application of being able to accurately and efficiently measure the distribution of path-lengths. This scheme could be used, for example, to measure the variations of a potential field between different paths. More generally, these applications hint at the great possibilities that multipoint devices hold for a range of new quantum schemes.

Acknowledgment

This work was supported by the United Kingdom EPSRC (grant no. GR/S99297/01).

References

- [1] Holland M J and Burnett K 1993 *Phys. Rev. Lett.* **71** 1355
- [2] Huelga S F *et al* 1997 *Phys. Rev. Lett.* **79** 3865
- [3] Dunningham J A and Burnett K 2004 *Phys. Rev. A* **70** 033601
- [4] D'Ariano G and Paris M G 1997 *Phys. Rev. A* **55** 2267
- [5] Vourdas A and Dunningham J A 2005 *Phys. Rev. A* **71** 013809
- [6] Reck M, Zeilinger A, Bernstein H J and Bertani P 1994 *Phys. Rev. Lett.* **73** 58
- [7] Torma P, Stenholm S and Jex I 1995 *Phys. Rev. A* **52** 4853
- [8] Jex I, Stenholm S and Zeilinger A 1995 *Opt. Commun.* **117** 95
- [9] Mattle K, Michler M, Weinfurter H, Zeilinger A and Zukowski M 1995 *Appl. Phys. B* **60** S111
- [10] Pryde G J and White A G 2003 *Phys. Rev. A* **68** 052315
- [11] Orzel C, Tuchman A K, Fenselau M L, Yasuda M and Kasevich M A 2001 *Science* **291** 2386
- [12] Greiner M, Mandel O, Esslinger T, Hansch T W and Bloch I 2002 *Nature* **415** 39
- [13] Kok P and Braunstein S L 2001 *Phys. Rev. A* **63** 033812
- [14] Fiurášek J 2002 *Phys. Rev. A* **65** 053818
- [15] Lim Y L and Beige A 2005 *Phys. Rev. A* **71** 062311
- [16] Winter J 2001 *J. Phys. A: Math. Gen.* **34** 7095
- [17] Buhrmann H, Cleve R, Waltrous J and de Wolf R 2001 *Phys. Rev. Lett.* **87** 167902
- [18] Andersson E, Barnett S M and Jex I 2003 *J. Phys. A: Math. Gen.* **36** 2325
- [19] Gradshteyn I S and Ryzhik I M 2000 *Tables of Integrals, Series, and Products* 6th edn (New York: Academic)